

## E. RELATIVISTIC HEAVY ION COLLISIONS

The PHOBOS experiment made significant advances over the past year, with the publication of several new results, the completion of the analysis of much of the data from the 2000 running cycle, and successful operation during the 2001 running period. Adding to the data obtained at  $\sqrt{s_{NN}} = 56$  and 130 GeV, PHOBOS obtained a number of new results for collisions at  $\sqrt{s_{NN}} = 200$  GeV, as well as some data taken at a low energy of  $\sqrt{s_{NN}} = 20$  GeV to establish a connection with the work done at the SPS at CERN. Finally, data were also obtained for polarized proton-proton collisions at  $\sqrt{s_{NN}} = 200$  GeV. These results provided many insights into the physics of these ultra-relativistic collisions, including the systematic dependence of charged-particle production on bombarding energy and impact parameter, the dynamics of charged particle production, baryon stopping and the temperature and chemical potential of the system.

### e.1. The PHOBOS Experiment at RHIC (B. B. Back, A. H. Wuosmaa, and the PHOBOS Collaboration - ANL, BNL, Krakow, MIT, NCU Taiwan, U. of Rochester, UIC, and U. of Maryland)

At RHIC, heavy ions collide at center of mass energies an order of magnitude higher than was previously available anywhere. At these energies, it is expected that a baryon-free region of extremely high energy density will remain in the central region after the two colliding nuclei have passed through each other. It is believed that this situation will be more than sufficient to create a system of deconfined quarks and gluons- the "Quark Gluon Plasma." After formation, the plasma should expand and cool before passing into the normal hadronic phase that, in turn, expands further until the hadrons cease to interact with each other ("freezeout"). The important questions that need to be answered are: what are the direct probes and signatures of the plasma phase, and what identifiable traces of the quark-gluon phase remain in the observed hadronic final state? The PHOBOS experiment seeks answers to these questions.

The PHOBOS experiment focuses on measurements of hadronic observables for a large sample of events. The PHOBOS apparatus consists of a  $4\pi$  multiplicity detector and two multi-particle tracking spectrometers capable of measuring and identifying particles with very low transverse momenta. The multiplicity detector can provide event-by-event charged particle multiplicity distributions, which will be used to find interesting events for study in more detail using the spectrometers. The multiplicity distributions are interesting in their own right, and contain information on fluctuations and correlations, which relate to some of the proposed signatures of the plasma. The multiplicity distributions also contain information about the dynamic evolution of the collision.

An overall view of the PHOBOS apparatus as it was installed for the Year 2001 Physics run is shown in Fig. I-52; several different components are identified. The apparatus is now complete with the installation of the second of the two tracking-spectrometer arms, which was completed in early 2001. The fabrication and installation of the multiplicity and vertex detectors was the responsibility of the groups at Argonne and UIC. Together, these systems contain over 22000 channels of silicon pad detector.

The Multiplicity detector provides event-by-event information on the charged particle multiplicity distributions over  $\pm 5.4$  units of pseudo-rapidity ( $\eta$ ), with complete azimuthal coverage. The multiplicity measurement (see results below) is made using a centrally located, 11000 channel "Octagon" array of silicon pads supplemented with six 512 channel "Ring" counters placed up and down the beam pipe. These detectors measure the energy deposited as a function of angle with respect to the collision vertex.

The Vertex detector is designed to locate the position of the interaction vertex on an event-by-event basis. It is composed of two pairs of planes of silicon pad detectors, each plane segmented into 2048 channels so that the occupancy is low. Particles emitted from the collision vertex can be tracked by combining pairs of hits on the inner and outer Vertex planes such that the position of the reconstructed interaction point can be determined to a precision

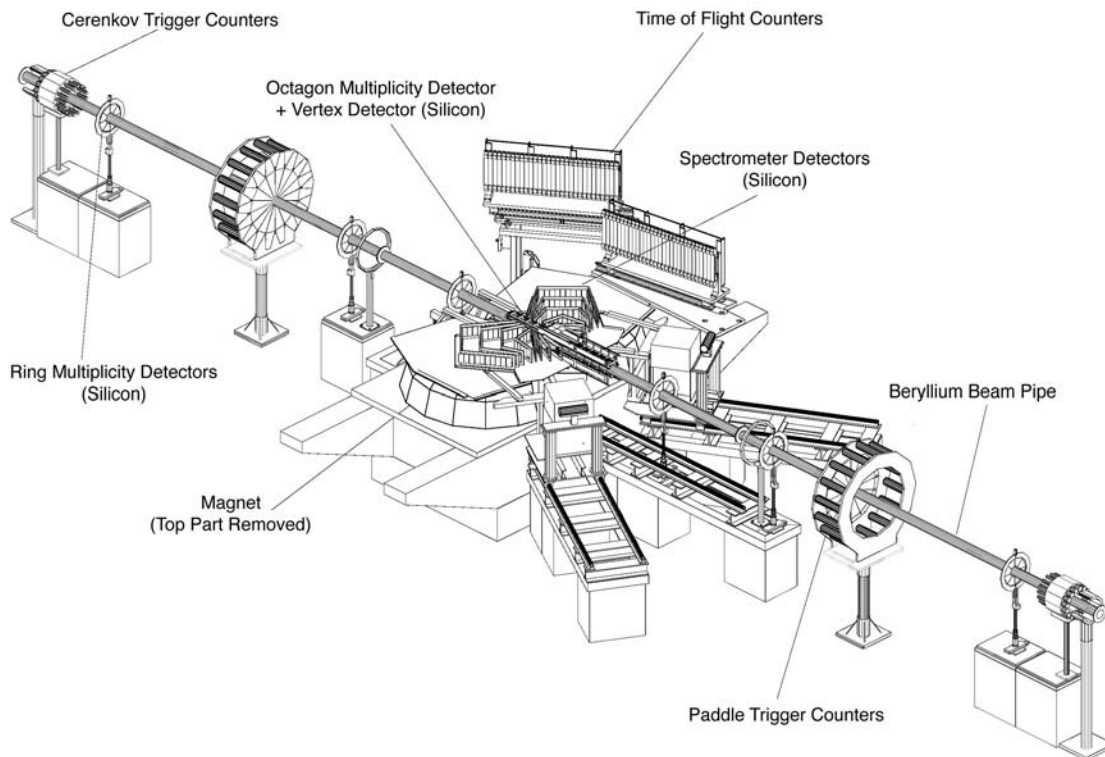


Fig. I-52. Overview of the PHOBOS experiment.

of better than 300  $\mu\text{m}$ . Vertices are reconstructed over the entire range of the RHIC collision diamond, nominally corresponding to  $\pm 20$  cm about the center of the intersection region.

#### Installation, Performance and Operation during 2001

As mentioned above, in the spring of 2001 the second spectrometer arm was installed, doubling the efficiency for tracking and identification of charged particles emitted at mid-rapidity. Also, the performance of the data acquisition (DAQ) was improved, yielding better stability and functionality than in the previous year. The apparatus continues to function well.

Au + Au operations at RHIC at  $\sqrt{s_{NN}} = 200$  GeV commenced in July 2001, and continued through November. Throughout this period, 56 of the possible 60 beam-bunches were filled, with an average intensity of many times  $10^9$  ions circulating per fill. The initial design luminosity goals for the accelerator were approached, and all of the RHIC experiments accumulated over an order of magnitude more data than in the previous years running.

Throughout the entire running period, frequent measurements of the noise and gain calibration of the entire PHOBOS system were taken to monitor the stability of the detectors. The noise, and hence the response of the detector were remarkably stable, with observed variations less than 2% throughout this period. The variations in the measured gain response for this period were similarly small. The total fraction of non-functioning channels was less than 3% out of the total 13700 channels installed.

Some difficulty was encountered during two incidents when control of the Au beams was lost, and large radiation fluxes were incident on the experiment. In these cases, the FEE protection circuits were overwhelmed and some degraded performance of some of the ASICS FEE chips was observed. Fortunately, by modifying the operating parameters of the affected chips, nominal operation of the detector was restored and the radiation incidents did not significantly affect the ultimate performance of the detector.

One additional improvement to the operation of the detector was the implementation of selective triggering. During most of the 2000 running period, data were taken with an effectively minimum-bias trigger, requiring only timing cuts on data from the plastic-

scintillator trigger detectors to signify a valid event. With the large increase in collision rates that accompanied the luminosity improvements from the accelerator, the minimum bias event rate increased from several 10 s of Hz in 2000, to as much as 1000 Hz. To enhance the fraction of the most interesting events from collisions in the central region of the detector, and from the most central collisions, a new triggering scheme was implemented. This scheme enhanced the fraction of good analyzable events by nearly an order of magnitude relative to the minimum bias trigger.

### Physics results

#### Systematic behavior of charged particle production at mid-rapidity:

#### Energy Dependence

The most straightforward observable quantities from energetic heavy-ion collisions involve the number and distribution of the emitted charged particles. These quantities are of particular interest as they are sensitive to all processes contributing to particle production, and serve as measures of the energy, and entropy densities

achieved during the collision. The PHOBOS experiment has a number of elements designed to study the charged-particle multiplicity from such collisions. One of the earliest and most fundamental questions about charged-particle production in heavy-ion collisions concerns the energy dependence of  $dN_{ch}/d\eta$  at mid-rapidity.

The first measurements of charged particle production from relativistic Au + Au collisions at RHIC were reported from the PHOBOS experiment,<sup>1</sup> from data obtained during the commissioning phase of RHIC running in June 2000. These first measurements were confined to the most central collisions, for particles emitted in the mid-rapidity region ( $|\eta| < 1$ ). Additional data from  $\sqrt{s_{NN}} = 200$  GeV were reported.<sup>2</sup> The pseudo-rapidity density was determined by counting “tracklets” – tracks measured in the partial spectrometer arm or vertex detector that connect either hits in two of the 6 spectrometer planes, or the two vertex detector planes, with the reconstructed vertex position. After corrections are applied for detector acceptance, and the effects of secondary particle production and combinatorial background, the pseudo-rapidity density  $dN_{ch}/d\eta(|\eta| < 1)$  can be determined.

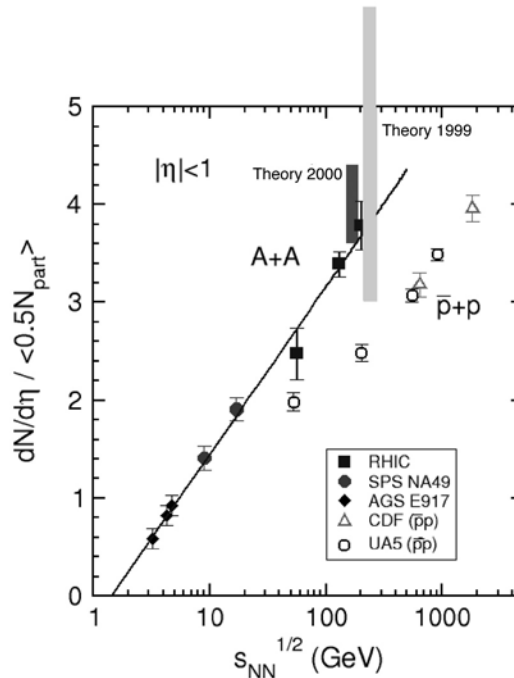


Fig. I-53. Bombarding energy dependence of charged particle production. The PHOBOS points are the solid squares.

Figure I-53 shows the measured bombarding energy dependence of the charged-particle pseudo-rapidity density at mid rapidity for the 6% of the most central collisions, divided by the number of nucleon pairs participating in the collision ( $N_{pp} = 1/2 N_{part}$ ). For comparison, data at lower energies from the AGS<sup>3</sup> and CERN SPS Pb + Pb program<sup>4</sup> are also shown. The heavy-ion data show a logarithmic increase with bombarding energy. Compared to proton-antiproton scattering<sup>5</sup> the charged particle density per participant nucleon-nucleon pair is as much as 70% higher for the heavy-ion system as compared to proton-antiproton collisions. This enhancement clearly indicates that charged-particle production at mid rapidity in the heavy-ion system reflects process beyond simple nucleon-nucleon scattering. These data also provide significant constraints on theoretical predictions for such collisions. The bar labeled “Theory 1999” shows the range of theoretical predictions for  $dN_{ch}/d\eta$  at mid rapidity before Au + Au operations began at RHIC. This range was tightly restricted by our  $\sqrt{s_{NN}} = 56$  and 130 GeV data (bar labeled “Theory 2000”). The  $\sqrt{s_{NN}} = 200$  GeV data point lies at the lower edge of the range of the “Theory 2000” bar.

#### Centrality dependence of $dN_{ch}/d\eta$ at $\eta = 0$ :

A measurement of the impact parameter, or centrality, dependence of  $dN_{ch}/d\eta$  is sensitive to the relative

contributions of hard (parton-parton) and soft (nucleon-nucleon) scatterings. With increasing energy, the collisions probe shorter distances and hard collisions are expected to have a greater influence. Also, different theoretical pictures yield differing contributions of hard and soft scatterings. Generally, particle production from soft nucleon-nucleon is expected to depend linearly on the number of participating nucleon-nucleon pairs ( $N_{part}/2$ ), while for hard collisions  $dN_{ch}/d\eta$  is expected to depend approximately linearly on the number of nucleon-nucleon collisions, which approximately follows  $N_{part}^{4/3}$ . A measurement of  $dN_{ch}/d\eta$  vs  $N_{part}$  can provide information about this division.

Figures I-54(a) and (b) show  $(dN_{ch}/d\eta)/(N_{part}/2)$  plotted versus the number of participating nucleons  $N_{part}$ , for  $\sqrt{s_{NN}} = 130^6$  and 200 GeV. The systematic uncertainty of approximately 6% was determined by comparing the results from different detector systems. Also plotted are the predictions from HIJING,<sup>7</sup> saturation models,<sup>8</sup> and from more empirical fits to the data assuming a combination of hard and soft scatterings.<sup>9</sup> The data do not support either the HIJING or saturation pictures, and in fact fall somewhere in between the two. The hard/soft fits do a better job, with the contribution of hard scattering increasing from approximately 9% to 11% with increasing bombarding energy.

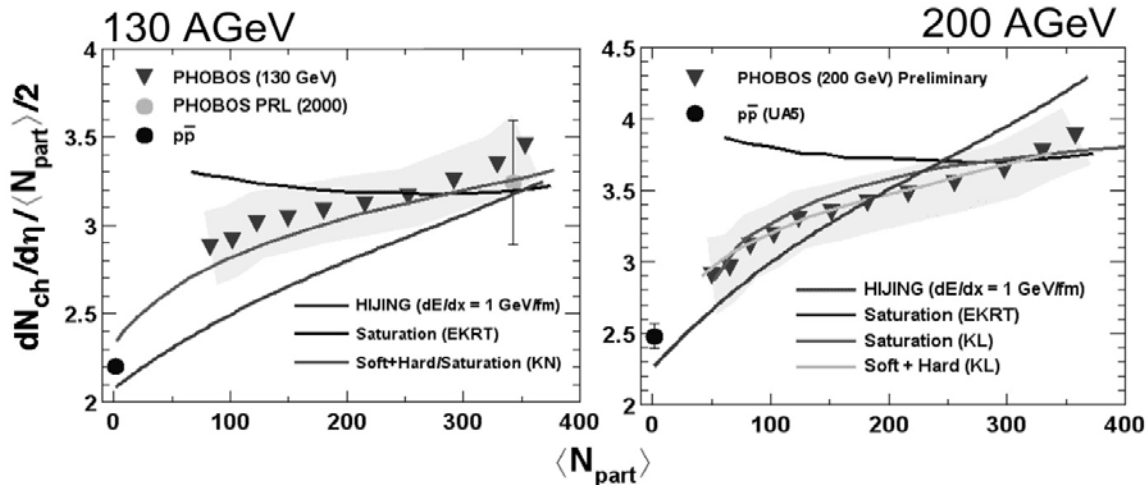


Fig. I-54. Centrality dependence of charged-particle production for central collisions at mid rapidity at  $\sqrt{s_{NN}} = 130$  (a) and 200 (b) GeV.

$4\pi dN_{ch}/d\eta$ :

Further information may be obtained by studying the pseudo-rapidity dependence of  $dN_{ch}/d\eta$ . This measurement was performed using the multiplicity detectors that were constructed by the Argonne-UIC group. This multiplicity measurement is completely independent of the tracklet analyses described above. Two methods were used to study  $dN_{ch}/d\eta(\eta)$ . One method relies on counting the hit pads in the multiplicity detector, as a function of pseudorapidity. The number of hit pads is corrected for the acceptance, as well as the effects of detector occupancy, secondary particle production, weak decays, and background. The background corrections were made using a comparison to a Monte Carlo simulation of the detector. The alternative method involves measuring the total energy deposited in the multiplicity detector  $\Delta E(\eta)$  as a function of pseudorapidity. The measured deposited energy is then compared to the average energy

deposited by a charged particle vs pseudorapidity, and corrected for contributions of background, also carried out using a Monte Carlo simulation. The two methods provided results that were in excellent agreement with each other.

The measured distributions of  $dN_{ch}/d\eta$  at  $\sqrt{s_{NN}} = 130$  GeV for several centrality bins appear in Fig. I-55.<sup>10</sup> The centrality dependence of these data appears in Fig. I-56, where the panels (b) - (f) represent data taken at various values of  $\eta$ . Figure I-56(a) shows the integrated charged-particle yield as a function of centrality. For the most central collisions, we measure a total of approximately 4200 charged particles produced within  $|\eta| < 5.4$ . In most cases the data are not well reproduced by the calculations with the HIJING code (solid lines). Other models<sup>11,12</sup> which include hadronic rescattering are better able to reproduce the data for large values of  $|\eta|$ .

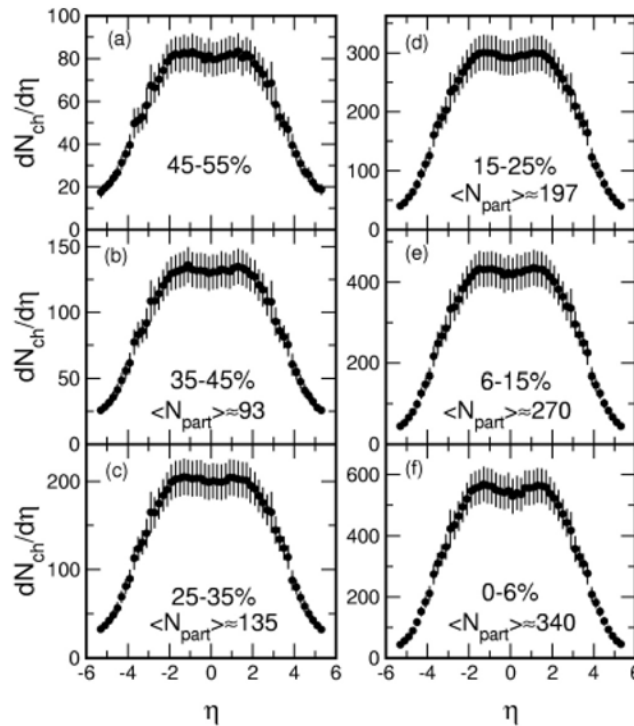


Fig. I-55.  $dN_{ch}/d\eta$  vs.  $\eta$  for various collision centralities.

Figure I-57(a) shows a comparison between the distributions of  $dN_{ch}/d\eta/(N_{part}/2)$  for the 6% most central collisions at  $\sqrt{s_{NN}} = 130$  and 200 GeV. Figure I-57(b) compares the 200 GeV central Au + Au data with data from proton-antiproton scattering at that energy. The enhancement of charged-particle

production at mid rapidity is clear, however at larger values of  $|\eta|$  the two data sets are closer to each other, perhaps suggesting that charged particle production for  $|\eta| > \sim 3$  may be governed by simpler mechanisms following nucleon-nucleon scattering.

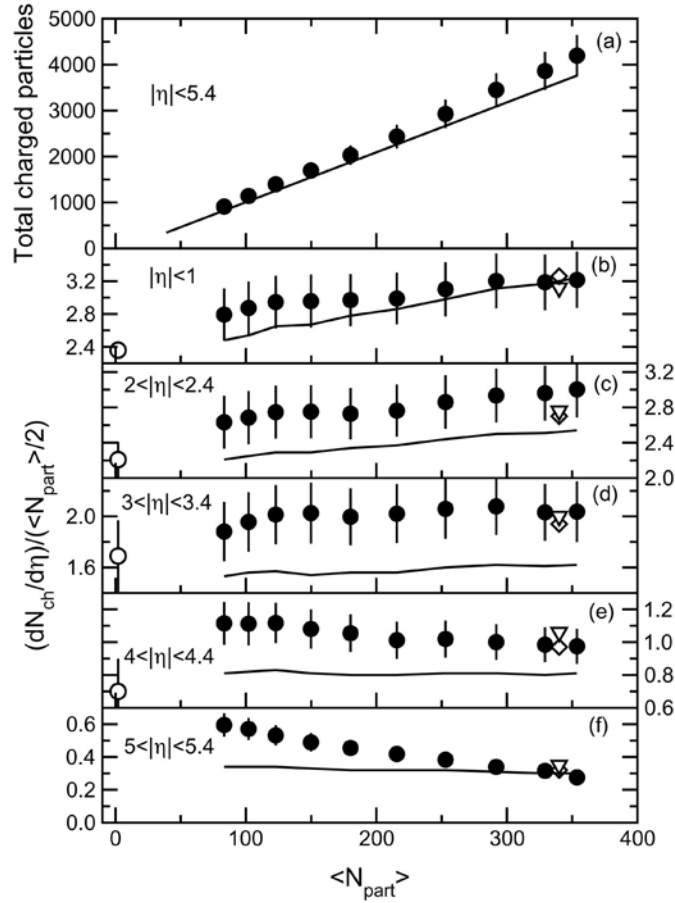


Fig. I-56. Centrality dependence of (a) total charged-particle production for  $|\eta| < 5.4$  and (b - f)  $dN_{ch}/d\eta$  at various values of  $\eta$ . The solid curves represent calculations using the HIJING model.

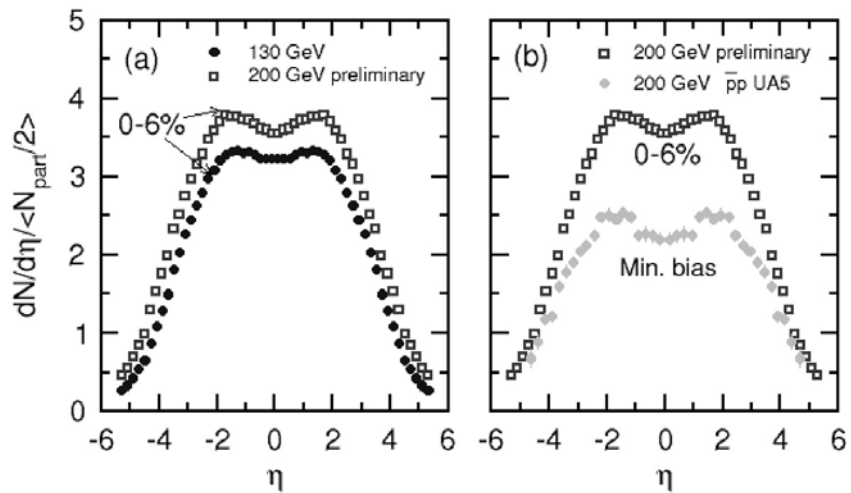


Fig. I-57. (a)  $dN_{ch}/d\eta$  vs  $\eta$  for central collisions at  $\sqrt{s_{NN}} = 130$  GeV (solid circles) and 200 GeV (open squares). (b) Central  $dN_{ch}/d\eta$  for Au + Au (open squares) and  $\bar{p}p$  (solid circles) collisions at  $\sqrt{s_{NN}} = 200$  GeV.

Evidence in favor of this view may be supported by a comparison between, for example, the data for central collisions at  $\sqrt{s_{NN}} = 130$  and 200 GeV, when viewed in the rest frame of one of the colliding nuclei. When plotted as a function of the so-called “shifted pseudorapidity”  $\eta' = \eta - y_{BEAM}$ , where  $y_{BEAM}$  is the

beam rapidity. Here, for values of  $\eta' < 2$ , the two sets of data lie virtually on top of each other. This behavior is reminiscent of the phenomenon called “limiting fragmentation” which is well known in proton-proton and proton-nucleus scattering (see, for example, Fig. I-58(a)).

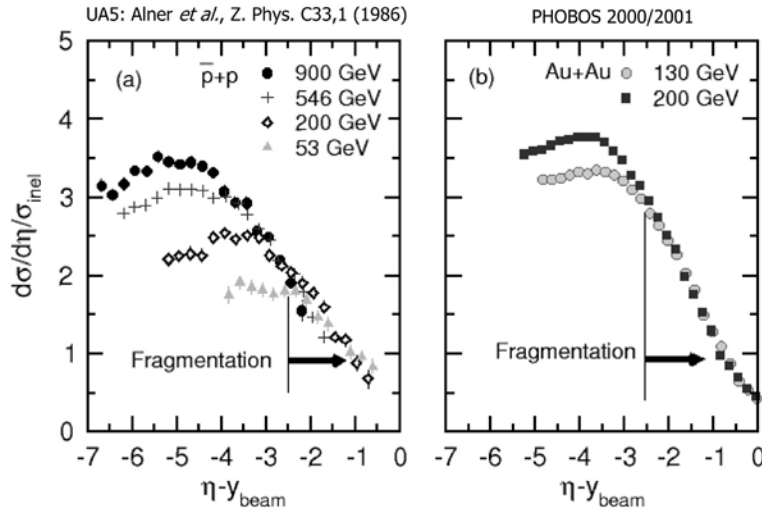


Fig. I-58. (a) Distributions of  $dN_{ch}/d\eta$  vs  $\eta' = \eta - y_{BEAM}$  from  $\bar{p}p$  scattering at different energies. (b)  $dN_{ch}/d\eta$  vs  $\eta'$  from Au + Au collisions at  $\sqrt{s_{NN}} = 130$  (circles) and 200 GeV (squares).

#### Baryon density at mid rapidity:

One prediction of the situation achieved in heavy-ion collisions at highly relativistic energies is that the two nuclei pass through each other, leaving a very hot, but essentially baryon free, region between them from which particles and anti-particles are produced. In order to determine whether this central region is actually baryon-free, it is useful to study the ratio of anti-baryons to baryons at mid-rapidity. If the participant baryons carried within the colliding nucleons are indeed swept out of the hot central zone, then the ratio of the numbers of observed baryons, and anti-baryons at mid-rapidity should be approximately unity. Furthermore, this ratio may be related to the amount of kinetic energy transformed into energy available for particle production.

The ratio of anti-protons to protons at mid rapidity was measured in PHOBOS using data from the tracking spectrometer with the magnet energized to its full field value of 2T. Tracks were analyzed by first identifying straight tracks in the 6 spectrometer planes within the field-free region near the beam pipe. These tracks were followed into the magnetic field region and then

momentum analyzed by comparing hits in the remaining spectrometer planes with predetermined patterns in a look-up table. The particles were identified by a measurement of their differential energy loss in the spectrometer planes. In order to address systematic uncertainties, data obtained with the two magnet polarities were compared. The different acceptances for positively and negatively charged species obtained with the two polarities effectively cancel. The results for  $\bar{p}/p$  and  $K^-/K^+$  are shown in Fig. I-59(a),<sup>13</sup> with data from Au + Au collisions at lower energies from the AGS, and from Pb + Pb collisions at the SPS. The value of  $\bar{p}/p = 0.6$  is somewhat less than one, implying that the mid-rapidity region is not yet entirely baryon free. The measured value is, however, approximately six times larger than that observed in Pb + Pb collisions at the SPS. The  $\bar{p}/p$  ratio is expected to more closely approach unity as the collision energy is increased to  $\sqrt{s_{NN}} = 200$  GeV in the RHIC 2001 physics run.

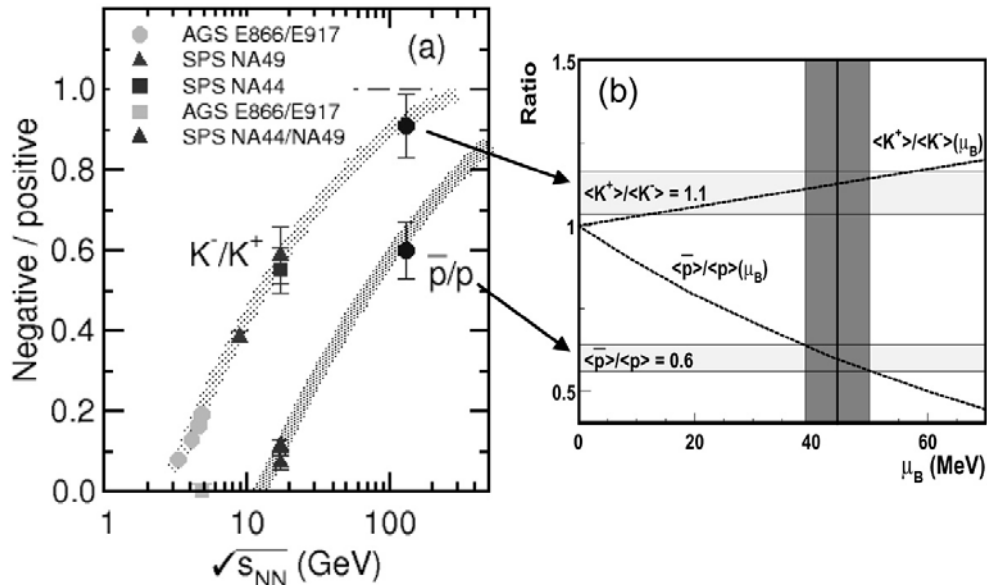


Fig. I-59. (a) Bombarding energy dependence of anti-particle/particle ratios. (b) Thermal model prediction of Redlich.<sup>14</sup>

The combined  $\bar{p}/p$  and  $K^-/K^+$  ratios can be used to infer the temperature and baryon chemical potential of the system. Figure I-59(b) shows a calculation by Redlich<sup>14</sup> performed in a thermal model. The horizontal bands represent the measured values of the anti-particle/particle ratios. Within the context of this

model, the data for  $\sqrt{s_{NN}} = 130$  GeV are consistent with a baryon chemical potential  $\mu_B = 45$  MeV, and a temperature of approximately 165 MeV. These values are within the range where quark and gluon degrees of freedom are expected to become important.

<sup>1</sup>B. B. Back *et al.*, Phys. Rev. Lett. **85**, 3100 (2000).

<sup>2</sup>B. B. Back *et al.*, Phys. Rev. Lett. **88**, 022302 (2002).

<sup>3</sup>B. B. Back *et al.*, Nucl. Phys. **A661**, 690 (1999).

<sup>4</sup>J. Bachler *et al.*, Nucl. Phys. A **661**, 45 (1999).

<sup>5</sup>F. Abe *et al.*, Phys. Rev. D **41**, 2330 (1990).

<sup>6</sup>B. B. Back *et al.*, Phys. Rev. C, **88**, 031901(R) (2002).

<sup>7</sup>X. N. Wang and M. Gyulassy, Phys. Rev. D **44**, 3501 (1991).

<sup>8</sup>K. J. Eskola *et al.*, Nucl. Phys. B **570**, 379 (2000).

<sup>9</sup>D. Karzhev and M. Nardi, Preprint nucl-th/0012025.

<sup>10</sup>B. B. Back *et al.*, Phys. Rev. Lett. **87**, 102303 (2001).

<sup>11</sup>Z. Lin *et al.*, Preprint nucl-th/0011059.

<sup>12</sup>D. E. Kahana and S. H. Kahana, Phys. Rev. C **59**, 1651 (1999).

<sup>13</sup>B. B. Back *et al.*, Phys. Rev. Lett. **87**, 102301 (2001).

<sup>14</sup>K. Redlich, Proceedings of the 15th International Conference on Ultra-relativistic Heavy Ion Collisions, (2001).